Vibration prediction of thin-walled composite I-beams using scaled models

Mohamad Eydani Asl*, Christopher Niezrecki, James Sherwood, Peter Avitabile

Department of Mechanical Engineering, University of Massachusetts Lowell, One University Avenue, Lowell, Massachusetts 01854

Abstract

Scaled models of large and expensive structures facilitate in understanding the physical behavior of the large structure during operation but on a smaller scale in both size and cost. These reduced-sized models also expedite in tuning designs and material properties, but also could be used for certification of the full-scale structure (referred to as the prototype). Within this study, the applicability of structural similitude theory in design of partially similar composite structures is demonstrated. Particular emphasis is placed on the design of scaled-down composite I-beams that can predict the fundamental frequency of their corresponding prototype. Composite I-beams are frequently used in the aerospace industry and are referred to as the back bone of large wind turbine blades. In this study, the governing equations of motion for free vibration of a shear deformable composite I-beam are analyzed using similarity transformation to derive scaling laws. Derived scaling laws are used as design criteria to develop scaled-down models. Both complete and partial similarity is discussed. A systematic approach is proposed to design partially similar scaled-down models with totally different layup from those of the full-scale I-beam. Based on the results, the designed scaled-down I-beams using the proposed technique show very good accuracy in predicting the fundamental frequency of their prototype.

Keywords: Wind turbine blade, Similitude, Sub-component, Composite I-beam, Distorted layup scaling

1. Introduction

The certification process for a wind turbine blade starts with coupon testing of the materials that are used in the manufacture of the blade and is finalized with full-scale testing of the blade. Coupon testing is relatively quick and cost-effective, but it is not fully representative of the structural integrity of the blade. In contrast, full-scale testing is time consuming and very expensive (e.g. hundreds thousands of dollars). As blade lengths continue to increase, the logistics of full-scale testing become more challenging and the test time increases as the resonant frequency of the blade decreases. Therefore, the total time for doing a specific number of fatigue cycles increases. Subcomponent testing can bridge the gap between coupon and full-scale testing of the blade. If meaningful scaled-down models can be designed that are representative of their parent components in the full-scale blade, then blade certification can be expedited and the confidence of blade manufacturers for introducing new materials (e.g. bio-based resins) into the industry can grow.

Interest and activity in the testing of wind-turbine-blade subcomponents has gained momentum in recent years and this interested has led to a number of case studies of a variety of parts of utility-scale wind turbine. Mandell et al. [1] tested composite I-beams with flanges and shear webs out of components which are used in the cross section of wind turbine blades. Stiffness and strain measurements that were observed in a four-point bending test of the beams were in agreement with predictions from simple beam theory and finite element analysis. Cairns et al. [2] studied the root section of the blade where the root specimens represented a single insert of a blade root into the hub joint. The primary focus of the study was manufacturing, but a significant amount of static and fatigue strength data were generated by performing pull-out tests. Mandell et al. [3] conducted a study with the focus on skin-stiffener intersections and sandwich panel closeout. Their goal was to predict skin-stiffener fracture loads and evaluate performance at locations where the sandwich panel transitions into the normal laminate.

A few studies investigated the performance of adhesive joints and bond lines of a wind turbine blade using subcomponent testing. The idea was to test the static and fatigue properties of the shear web to spar cap bond under stress states that are representative of those seen during field service of a wind turbine blade. Sayer et al. [4] proposed an asymmetric three-point bending test where they used a custom beam configuration which has come to be called a Henkel beam. It was meant to give a comparable

* Corresponding author. Tel.: +1 978 934 2584; fax: +1 978 934 3048.
E-mail addresses: Mohamad_Eydaniasl@student.uml.edu (M. E. Asl), Christopher_Niezrecki@uml.edu (C. Niezrecki), james_sherwood@uml.edu (J. Sherwood), Peter_Avitabile@uml.edu (P. Avitabile).

combination of bending moment and shear forces as a three-point bending test while reducing the stress concentrations at the clamped end. The specimen was used for a parametric study, investigating the influence of the design and manufacturing variables on shear web to spar cap adhesive joints [5]. Zarouchas et al. [6] performed a static four-point bending test on two symmetric I-beams. The tested I-beams represented the spar cap and shear web structure inside a wind turbine blade.

Although subcomponent testing is usually categorized as laboratory-scale test rigs, there are a few mid-level blade test approaches that fall into the subcomponent category. Jensen [7] conducted a study of the structural static strength of a box girder of a 34-m wind turbine blade, loaded in flap-wise direction. A combination of experimental and numerical work was used to address the critical failure mechanisms of the box girder of wind turbine blade. White et al. [8] developed a dual-axis test setup on a truncated 37-m wind turbine blade which combined resonance excitation with forced hydraulic loading to reduce the total test time required for evaluation. Subcomponents in this category are known as "Designed Subcomponents". Such subcomponents provide an accurate evaluation of the structural performance of the blade and can be used to characterize the dominant failure modes. However, such tests are involved, expensive and hard to implement on a laboratory scale.

The designed subcomponent (referred to as the "model") regardless of the size and complexity needs to be correlated with the full-scale component (referred to as the "prototype", see Fig.1). The connection between the scaled model and the prototype must be based on the structural parameters that predict the behavior of the system under consideration. Similitude theory can extract scaling laws from the governing equations of the system to connect the response of the scaled-down model to the prototype. To take advantage of the scaling laws, a properly scaled model should be designed to work well with the derived scaling law. In other words, the designed scaled model should be able to predict the response the prototype accurately by using the derived scaling laws. Otherwise, the experimental data of the scaled model cannot be correlated with the prototype, and therefore, the designed model cannot be representative of its corresponding prototype. As the model is not always an exact scaled-down replica of the prototype, a logical methodology should be implemented to design scaled models that can be used with scaling laws to predict the response of the prototype.

Similitude theory is an analytical tool for determining the necessary and sufficient conditions of similarity between two systems. These similarity conditions may be derived directly from the governing equations of the system which lead to more specific similarity conditions than dimensional analysis. Simitses and Rezaeepazhand [9] established a technique that could be applied directly to the governing equation of a system to derive the scaling laws. The derived scaling laws are then used to predict or estimate the response of a prototype by the response of its associated model. The buckling response of an orthotropic and symmetric cross-ply laminated plate was investigated as a benchmark in that study. In later studies, they analyzed the vibration of scaled laminated rectangular plates [10]. Additionally, they studied the effect of axial and shear load on stability of scaled laminated rectangular plates [11, 12]. According to their results, the scaling laws that are obtained directly from the governing equations can be used with perfect accuracy for cross-ply laminates, while for the angle-ply laminates the scaling laws did not show good accuracy. Later, this method was extensively used in their works regarding the vibration response of laminated shells [13, 14].

The design of scaled models for a structure made of composite materials is more challenging than the same structural shape made of isotropic materials. Laminated structures cannot be scaled down to any arbitrary size because of the practical difficulties in scaling the thickness of the plies of a laminate. Design of scaled-down composite models with the same layup as the prototype will be limited by manufacturing constraints because only fabrics with specific thicknesses are available in industry. Therefore, making scaled-down composite models with a completely similar lamination scheme as the prototype is hard to implement. Therefore, use of partially similar scaled models can be considered as an alternative. Although ply-level scaling [9] within the scope of complete similarity has been implemented successfully, the design of partially similar models is still lacking a systematic methodology.

Within this study, which is an extension of Authors' previous work on design of scaled composite models [15-17], similitude theory is applied to the governing equations of motion for vibration of a thin-walled composite I-beam [18] to design scaled-down composite I-beams which are representations of the spar caps and shear web of a utility scale wind turbine blade [19]. This paper presents the first work to design partially similar laminated models with totally different layups than their prototype using a systematic approach to predict the vibration response of the prototype. The main strength of the proposed approach compared to the numerical assessments is that a representative scaled model can be used for validation of the numerical estimation of the structural parameters as numerical assessments require experimental validation. Use of the scaled-down models to assess the natural frequencies of the full-scale structure provides an inexpensive approach to validate the numerical estimation of the frequencies using experimental data prior to full-scale testing of the structure. However, the proposed approach has its own limitations in terms of the design and manufacturing of the scaled model. The design of the scaled model should follow a logical methodology to ensure the similarity between the model and the prototype. Moreover, the feasibility of manufacturing of the

designed model needs to be considered in the design procedure. Both of the mentioned limitations are analyzed carefully in this study to design the models that are similar to their prototype and practical to be manufactured. The models designed with the proposed approach are shown to have a very good accuracy in predicting the fundamental frequency of their corresponding prototype.

When combined into an I-beam, the spar caps and shear web constitute the backbone of wind turbine blades. Thus, they are a major structural component of the blade and make for an interesting case study for subcomponent test design. In this study, similitude theory is applied to the subcomponent test concept, to develop scaled-down models that are representative of the dynamic characteristics of the I-beam structure inside a utility-scale blade. Governing equations for vibration of a simply-supported thin-walled shear deformable composite I-beam are considered to derive the scaling laws. Derived scaling laws are used as design criteria to develop scaled models that can accurately predict the fundamental frequency of the prototype. Within this analysis, the geometry and ply scheme of the prototype were based on a portion of Sandia National Laboratories 100-m long wind turbine blade near the maximum chord. Both complete and partial similarity cases are studied based on the considered layup for the prototype. Models with different sizes and ply schemes are designed that can accurately predict the fundamental frequency of their corresponding prototype.

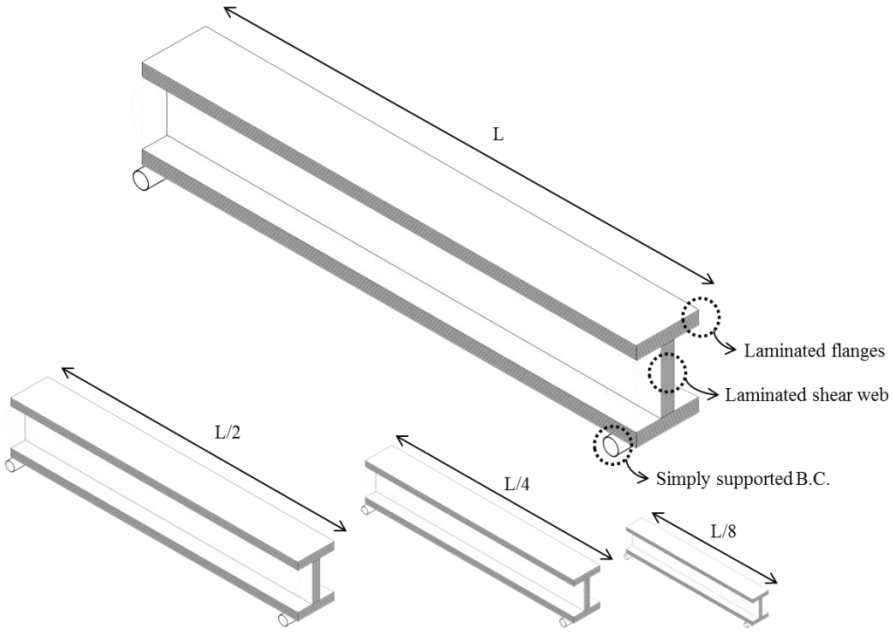

Fig. 1. Prototype (top) and Models with different scales and layups (bottom) showing the associated displacement boundary conditions.

2. Description of the mathematical model

This section presents the governing equations of motion for flexural vibration of a shear-deformable thin-walled composite I-beam shown in Fig. 2. The closed-form solution is derived for the natural frequencies of the I-beam with a simply-supported ends. Similarity transformation is subsequently applied to derive the scaling laws. The objective is to design scaled-down beams that can be used to predict the fundamental flexural frequency of the prototype using scaling laws. For this study, free vibration in the *y*-direction in the absence of thermal effects for a symmetric I-beam is considered.

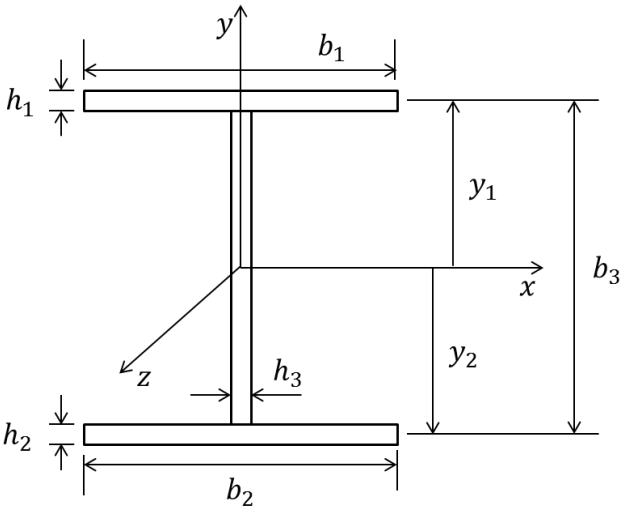

Fig. 2. Geometry of the I-beam and the associated reference frame [18].

A shear-deformable model was considered in this study as shear flexibility has a remarkable effect on natural frequencies of the laminated beams [20]. Neglecting all coupling effects due to the symmetric geometry, the equations governing free flexural vibration in *y*-direction are given by [18] and are the well-known Timoshenko beam equations:

$$(GA_x)_{com}(V'' + \Psi'_x) = \rho A\ddot{V} \tag{1a}$$

$$(EI_x)_{com}\Psi''_x - (GA_x)_{com}(V' + \Psi_x) = \rho I_x\ddot{\Psi}_x \tag{1b}$$

where Ψ_x denotes the rotation of the cross section with respect to *x* axis shown in Fig. 2, V the displacement in the *y* direction, the prime ($'$) is used to indicate differentiation with respect to *z* and the dot ($\dot{}$) is used to denote differentiation with respect time. The density and area of cross section are expressed by ρ and *A*, respectively, and I_x is the area moment of inertia with respect to the *x*-axes. The terms $(GA_x)_{com}$ and $(EI_x)_{com}$ are shear and flexural rigidity of thin walled composite ($_{com}$) with respect to the *x*-axis, respectively which could be expressed as:

$$(EI_x)_{com} = [A^{\alpha}_{11}(y_{\alpha})^2 - 2B^{\alpha}_{11}\, y_{\alpha} + D^{\alpha}_{11}]b_{\alpha} + \frac{(b_3)^3}{12}A^3_{11} \tag{1c}$$

$$(GA_x)_{com} = A^{\alpha}_{55}b_{\alpha} + A^3_{66}b_3 \tag{1d}$$

where $A_{11}, A_{66}, A_{55}, B_{11}$ and D_{11} are elements of extensional, coupling and bending stiffness matrices for a composite layup [21]. The repeated index α denotes summation where index α varies from 1 to 3 where the indices 1 and 2 represent the top and bottom flanges, respectively, and 3 is for the web, as shown in Fig. 2, and b_{α} denotes width of the flanges and web. Although employment of the in-thickness shear deformability may result in over-prediction of the frequencies specially for shorter beams and higher modes [22], considered model in this study was shown to predict the fundamental frequency of the I-beam geometry accurately and in good agreement with analytical solution and finite element results [18]. The closed-form solution for flexural natural frequencies in the *y*-direction may be directly calculated for the simple-support boundary condition as [18]:

$$\omega_{y_n} = \sqrt{\left[\frac{\rho A}{(EI_x)_{com}}\frac{L^4}{n^4\pi^4} + \frac{\rho A}{(GA_x)_{com}}\frac{L^2}{n^2\pi^2}\right]^{-1}} \tag{2}$$

where *n* indicates the mode number.

3. Scaling laws for vibration of composite I-beams

Natural frequencies for vibration of a simply supported shear-deformable composite I-beam are described by Eq. (2). To derive the scaling laws, it is assumed that all the variables of the governing equations for the prototype (x_p) can be connected to their corresponding variables in a scaled model (x_m) by a one-to-one mapping. Then, the scale factor for each variable can be defined

as $\lambda_x = x_p/x_m$ which is the ratio of each variable of the prototype to that of the scaled model. Rewriting Eq. (2) for the model and prototype and applying similarity transformation, the scaling laws can be extracted as follows based on the standard similitude procedure [9]:

$$\lambda_l{}^2 = \frac{\lambda_{EI}}{\lambda_{GA}} \tag{3}$$

$$\lambda_\omega = \sqrt{\frac{\lambda_n{}^4 \lambda_{EI}}{\lambda_\rho \lambda_A \lambda_l{}^4}} \tag{4a}$$

$$\lambda_\omega = \sqrt{\frac{\lambda_n{}^2 \lambda_{GA}}{\lambda_\rho \lambda_A \lambda_l{}^2}} \tag{4b}$$

Eq. (3) is referred to as the design scaling law and is a prerequisite for deriving the constitutive scaling laws Eq. (4a-b). Design scaling law Eq. (3) denotes that the ratio of the flexural rigidity to the shear rigidity must be equal to the square of the length of the two scales for complete similarity between two shear-deformable beams to exist. With Eq. (3) satisfied, the ratio of the natural frequencies between the two scales can be obtained using constitutive scaling laws Eq. (4a-b). Eq. (4a) predicts the natural frequencies of the prototype using the flexural stiffness ratio of the model and the prototype (i.e. λ_{EI}) while Eq. (4b) predicts the natural frequencies of the prototype using the shear stiffness ratio of the model and the prototype (i.e. λ_{GA}). However, if models are designed such that they satisfy Eq. (3) where $\lambda_l{}^2 = \lambda_{EI}/\lambda_{GA}$ then Eqs. (4a) and (4b) yield the same results in predicting the natural frequencies of the prototype. Upon expanding Eq. (3) by using the definition of the flexural and shear rigidities as provided in Eq. (1c-1b), specific design scaling laws can be written. For the specific case of assuming that the flanges and shear web of the I-beam are identical, Eq. (1b) and Eq. (1c) can be simplified as follows:

$$(EI_x)_{com} = 2A_{11}y^2 b - 4\,B_{11} y b + 3D_{11} b + \frac{A_{11} b^3}{12} \tag{5}$$

$$(GA_x)_{com} = 3A_{55} b + A_{66} b \tag{6}$$

The second term of Eq. (5) vanishes for a symmetric layup for the flanges and the web, i.e. $B_{11} \rightarrow 0$. Also the third term in Eq. (5) is negligible for a thin-walled beam, i.e. $D_{11} \rightarrow 0$. This study focuses on the fundamental frequency (n=1), but the same methodology can be utilized for the higher modes. Upon applying the similarity transformation to Eq. (5) and Eq. (6), the following scaling laws can be found:

$$\lambda_{EI} = \lambda_b \lambda_{A_{11}} \lambda_y{}^2 = \lambda_{A_{11}} \lambda_b{}^3 \tag{7}$$

$$\lambda_{GA} = \lambda_b \lambda_{A_{55}} = \lambda_b \lambda_{A_{66}} \tag{8}$$

By substitution of Eq. (7) and Eq. (8) into Eq. (3), the following scaling laws are derived for a symmetric thin-walled laminated I-beam:

$$\lambda_b = \lambda_y = \lambda_l \tag{9}$$

$$\lambda_{A_{11}} = \lambda_{A_{66}} = \lambda_{A_{55}} \tag{10}$$

Eq. (9-10) are specific versions of Eq. (3) which are valid for a thin-walled composite I-beam with a symmetric layup. To use the constitutive response scaling laws Eq. (4a-b) to predict the vibration frequencies of the prototype using a scaled model, Eqs. (9-10) must be valid between the prototype and the scaled model. Eq. (9) can be satisfied by assuming that that model and the prototype have the same geometrical aspect ratio. However, validation of Eq. (10) depends on the respective layup schemes of the prototype and of the model.

In the next sections of this study, validation of Eq. (10) is investigated by considering different layups for both prototype and scaled models. To have Eq. (9) satisfied for all the case studies, all models are assumed to have the same geometrical aspect ratio

as their corresponding prototype. Eq. (10) is then used as a design criterion to search through all possible model layups for a fixed prototype layup and to select the layups that completely or partially satisfy the terms of the equation. Finally, the fundamental vibration frequency of the prototype is predicted using the frequency of the models and response scaling laws Eq. (4a-b). In this study the scaling laws were derived for simply-supported boundary conditions however, the proposed approach is applicable to different boundary conditions (e.g. CC, SC, SF, CF and FF). For instance, the scaling laws for predicting the natural frequencies for clamped-clamped boundary conditions take the same form as Eqs. (3-4) however, the eigen values and natural frequencies are determined using numerical or approximate solutions.

4. Complete similarity

To achieve the complete similarity between the prototype and the model, all the scaling laws must be satisfied. In this case, the resulting model is a scaled replica of the prototype and theoretically can predict the response of the prototype exactly by using the constitutive response scaling laws. Based on the derived scaling laws, Eq. (9) and Eq. (10) must be satisfied to have complete similarity between the prototype and its corresponding scaled-down composite I-beam model. Eq. (9) is satisfied by the design of a model that has the same geometrical aspect ratio as its corresponding prototype. However, the satisfaction of Eq. (10) depends on the respective layup schemes of the model and of the prototype.

An equivalent ply-level description, e.g. $[(+\Theta_n/-\Theta_n)_s, n = 1,2,3,\dots]$, might be used to achieve complete similarity for laminated plate models in which the respective angles of the plies in the layup scheme of the laminate are denoted by Θ [14]. In this approach, the total number of the plies, i.e. n, with the same fiber angle Θ_n, is divided by an integer number that results in another integer that gives a model with the same extension, coupling and bending ratios as the prototype [15-16]. Ply-level scaling if applicable, yields models which automatically satisfy Eq. (10). Thus, to apply ply-level scaling and also achieve complete similarity, the prototype layup must have multiple plies for each fiber direction and the number of plies of each orientation must share a common integer factor.

The prototype geometry and the lay-up scheme considered in this study emulate the spar-cap flanges of the Sandia 100-m wind turbine blade [19] near the max chord. This area of the blade was chosen for analysis because many failures in blades occur near the max chord, and this area is of high of interest because it is responsible for carrying the majority of the aerodynamic loads.

For the current study, the prototype is assumed to be an I-beam consisting of three identical laminated plates having an overall dimension of 29.3 m × 2.446 m × 0.136 m with a layup of $[0]_{100}$ and ply thickness of t=1.36 mm. The taper along the length of the geometry of the full-scale component (i.e. first 1/3 of the Sandia blade from its root) was averaged to a constant cross-section to simplify the analysis. All computations are implemented for the glass/epoxy materials with the following material characteristics [19]: $E_1 = 41.8$ GPa, $E_2 = E_3 = 14$ GPa, $G_{12} = G_{13} = 2.63$ GPa, $G_{23} = 1.83$ GPa, $\upsilon_{12} = \upsilon_{13} = 0.28$, $\upsilon_{23} = 0.47$. Within this analysis, it was assumed that the geometry and layup scheme of the prototype was kept fixed while comparing to the models with various dimensions and ply stack up.

A unidirectional layup was assumed for the prototype, and scaled-down models were developed with the same geometrical aspect ratio as the prototype and unidirectional layup. The thickness of the plies for each of the models was considered to be fixed and to be the same as the prototype. The sizes of the developed models ranged from 1 to 100 plies in which the geometry and the layup of the largest model was identical to those of the prototype. All three of the terms in Eq. (10) have been plotted in Fig. 3 versus the ratio of the length of model to that of the prototype l_m/l_p when size of the models range from 1 to 100 plies assuming a prototype with the specified dimensions and unidirectional layup. The symbol l_m indicates the length of the model and l_p denotes the length of the prototype. Fig. 3 demonstrates that Eq. (10) is satisfied, meaning that all three extensional stiffness ratios among the different models and the prototype are equivalent. Validation of Eq. (3) for the developed models and the prototype as shown in Fig. 3 allows using response scaling laws as prescribed by Eq. (4a-b) to predict the frequency of the prototype. Because all of the models satisfy all of the necessary scaling laws for complete similarity which are Eq. (9) and Eq. (10), they can predict the fundamental vibration frequency of the prototype exactly using the constitutive response scaling laws Eq. (4a-b).

Next, the developed models are utilized to predict the theoretical fundamental frequency of the prototype. The constitutive response scaling laws as given by Eq. (4a-b) are applied to the frequency of the developed models to predict the theoretical vibration frequency of the prototype. Fig. 4 shows the overlapping of the predicted frequencies by each model to that of the prototype. This good correlation demonstrates excellent accuracies in prediction. The first bending mode resonant frequency is 8.23 Hz, and the models are able to predict this frequency by using the constitutive response scaling laws. Both of the response scaling laws Eq. (4a-b) yield the same results because all of the necessary conditions for complete similarity have been met by the developed models.

Although complete similarity holds between the developed models and the considered prototype, the use of ply-level scaling may not be applicable to design scaled models for a prototype with non-unidirectional layup. Direct ply-level scaling is limited to layups with multiple plies of a same angle. Also, the smallest scale model that can be designed through this approach is dictated by the ratio of the stacks of the angle plies in a given layup for a laminated plate. For example, consider the prototype with the ply stack up $[\pm 45_{\,2}/0_{\,46}]_s$ which is representative of a typical utility-scale blade layup for the spar caps. It is not possible to scale down the thickness to half of the prototype thickness using ply-level scaling because it will result in a non-integer number of plies. The design of partially similar models is considered an option only when complete similarity is not feasible. In the next section, a systematic methodology is developed to design scaled down composite I-beams that are partially similar to their corresponding prototype.

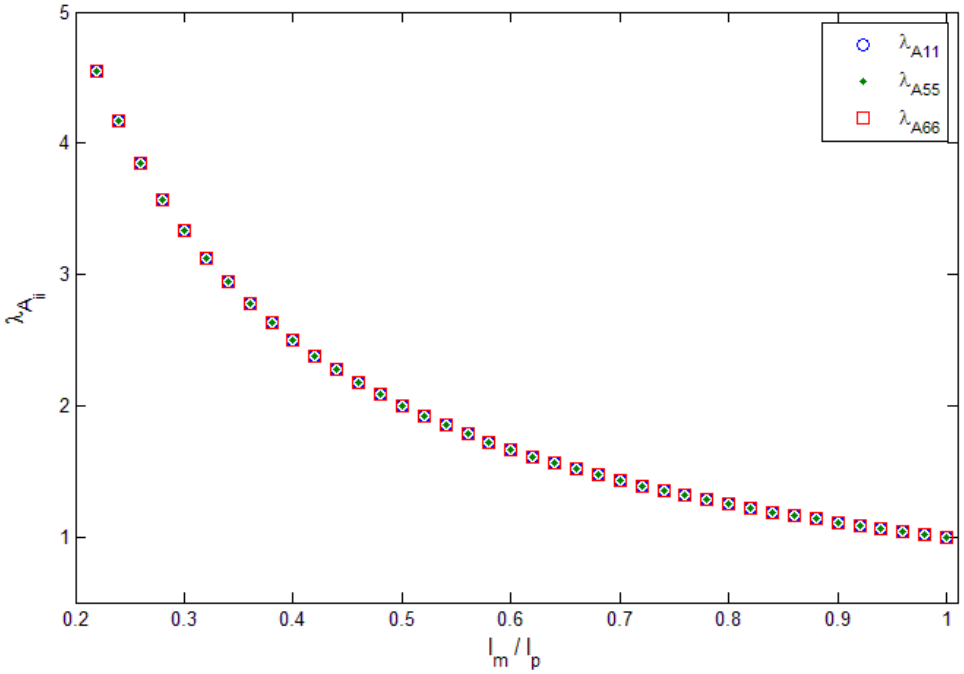

Fig. 3. Comparison of the terms in Eq. (10) as a function of the size of the model which demonstrates complete similarity.

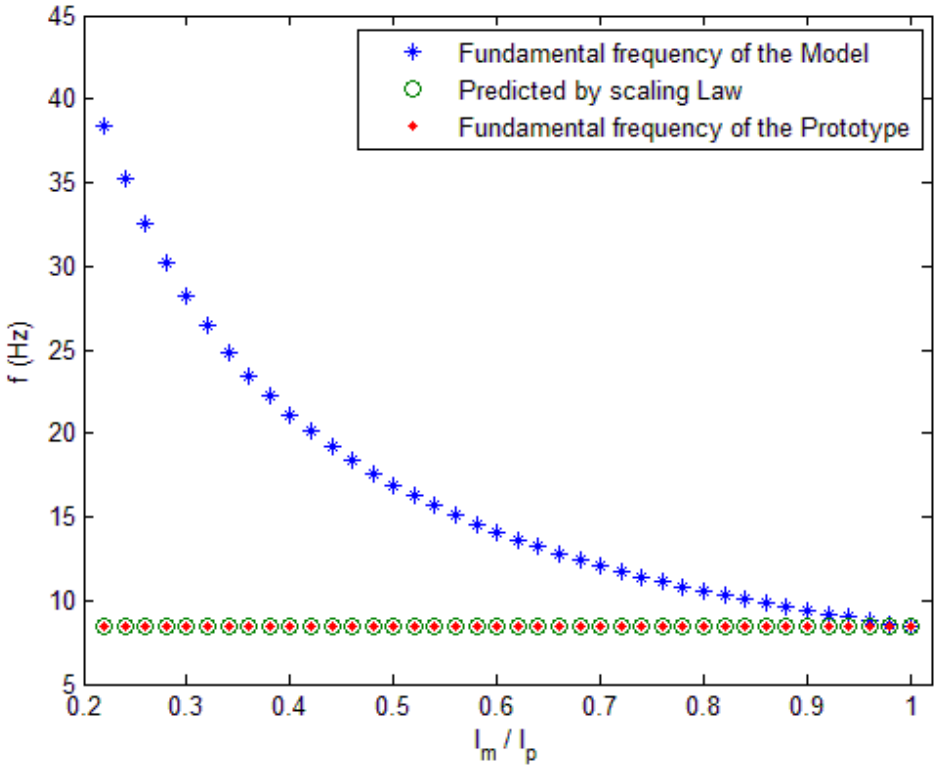

Fig. 4. Comparison of the predicted fundamental frequency of the prototype (green circles) to the actual frequency (red diamonds) by using the fundamental frequency of the model (blue stars) via the response scaling law for complete similarity.

5. Partial similarity

If satisfying all of the scaling laws between the model and the prototype is not applicable, then complete similarity is not feasible, and the analysis must accept that only partial similarity can be investigated. In partial similarity, some of the design scaling laws need to be relaxed to allow for the design of a scaled model. Although the partially similar model is not a scaled replica of its prototype, a designed model can be sufficiently accurate to capture the desired aspects of the prototype.

In the previous section, complete similarity was demonstrated for a composite I-beam with a unidirectional layup that was representative of the spar caps and shear web structure of a typical utility-scale wind turbine blade. To demonstrate the applicability of the scaled models for a more complex situation, two non-unidirectional layups with the same geometry are considered for the prototype. Scaled models with same geometrical aspect ratios as the prototype but with a distorted layup are developed to predict the dynamic behavior of the prototype. In this case, the scaling laws regarding the geometry of the models, i.e. Eq. (9), will be still be valid because all of models have the same geometrical aspect ratio as the prototype. However, for the developed models in this section, the scaling laws that are associated with the layup of the models in Eq. (10) are not completely satisfied. Discrepancy in the design scaling laws will result in error in prediction of the frequency using the constitutive response scaling laws Eqs. (4a-b). The goal is to find lamination layups for the model which lead to minimum error in prediction of the frequency of the prototype using appropriate response scaling laws.

5.1. Distorted layup scaling approach

To design a scaled laminated structure that is partially similar to its prototype, a common practice is to examine layups for the model that are similar to the layup of the prototype [12, 13]. However, the only condition that needs to be met to yield similarity between the model and the prototype is to satisfy the design scaling law. Any layup that fully or even partially satisfies the design scaling laws between the model and the prototype can be considered as a candidate layup for the model as long as the selected layup obeys the governing equations of the motion (e.g. balanced and symmetric in this case). This terminology admits a broad range of models to be available to designers and increases the probability of finding admissible models with smaller scales. To find layups that satisfy the design scaling laws and eventually yield sufficiently accurate partially-similar models, design scaling

laws can be rearranged and used as quantitative criteria to search through all possible layups for the model and to select the most accurate candidate models to predict the response of the prototype.

To design a partially-similar scaled down model with a distorted layup compared to the layup of the prototype, Eq. (10) is the only condition that needs to be approximately satisfied. Eq. (9) is already satisfied by assuming a geometrical aspect ratio for the model being the same as the prototype. Based on the prototype layup scheme, a permutation algorithm was implemented in the current research to identify the potential ply schemes for the model with an overall laminate thickness that is less than the thickness of the prototype and which approximately satisfies Eq. (10). Any ply scheme for the model that approximately satisfies Eq. (10) may be a candidate solution.

To demonstrate the feasibility of the proposed approach, two different non-unidirectional layups, i.e. $[\pm 45_{\,2}/0_{\,46}]_s$ and $[90_{\,2}/0_{\,46}]_s$, were considered for the prototype. These two ply schemes are more representative of a layup in a utility-scale wind turbine blade than a purely unidirectional layup previously explored. However, the majority of these two layups consist of the unidirectional plies which results in a very close flexural and shear stiffness values for both prototypes. The geometry of the prototype was kept the same as the previous section. The absolute-error criteria to find the desired layups based on satisfying design scaling laws in Eq. (10) were defined as:

$$e_1 = [(\lambda_{A_{55}} - \lambda_{A_{66}})/\lambda_{A_{66}}] * 100\% \tag{11-a}$$

$$e_2 = [(\lambda_{A_{11}} - \lambda_{A_{66}})/\lambda_{A_{11}}] * 100\% \tag{11-b}$$

Based on Eq. (10), the extensional stiffness elements A_{11}, A_{55} and A_{66} are critical factors in design of the scaled model for predicting the frequencies of the prototype. The ratios of the extensional stiffness elements in the model need to be equal to those of the prototype to accurately predict the frequencies of the prototype. To determine the degree of equivalency of the extensional stiffness ratios between model and prototype, two error criteria were defined. Eq. (11-a) is used as an error criterion to check the equivalency of the ratio of A_{55} and A_{66} between the model and the prototype. Similarly, Eq. (11-b) checks the equivalency of the ratio of the coefficients A_{11} and A_{66} between the model and the prototype.
To investigate the effect of each error criterion e_1 and e_2 on the total discrepancy in the design scaling law Eq. (3), the following error criterion was defined:

$$e = [(\frac{\lambda_{EI}}{\lambda_{GA}} - {\lambda_l}^2)/\frac{\lambda_{EI}}{\lambda_{GA}})] * 100\% \tag{12}$$

Rewriting Eq. (12) in terms of Eq. (7) and Eq. (8) and plugging Eq. (11-a) and Eq. (11-b) yields the following error criterion which includes both e_1 and e_2 criteria:

$$e = abs\ (e_2 - e_1 + e_1 e_2) * 100\% \tag{13}$$

A primary investigation of Eq. (13) shows that both e_1 and e_2 criteria participate in the total error in the design scaling law including the extensional stiffness ratios $\lambda_{A_{11}}$, $\lambda_{A_{66}}$ and $\lambda_{A_{55}}$.

5.2 Analytical observations

First, layup $[\pm 45_{\,2}/0_{\,46}]_s$ is considered for the prototype, and three different sets of models with different length scales are developed. Eqs. (11a-b) were used as the metric to select the most accurate layup for models with a given scale to predict the fundamental frequency of the prototype. For all the case studies, the error in satisfying the design scaling law Eq. (11a-b) is first examined, and then the fundamental frequency of the prototype is predicted using the constitutive-response scaling laws Eqs. (4a-b).

As the first benchmark for the distorted layup scaling technique, models with a total of 12 layers for each of the flanges and the web and $\lambda_l = 8.33$, i.e. 100 plies/12 = 8.33, were developed. The errors as defined by Eqs. (11a-b) for all of the possible symmetric and balanced 12-ply schemes with only include 0, 90 and ± 45 plies is shown in Fig. 5. The 0, 90 and ± 45 plies were selected intentionally to make the designed model easy to manufacture as these are the most commonly used orientations in practice. Among the 34 unique possibilities, the cases with permutation numbers 4, 5, 7, 10 and 16 were found to exhibit less than 30% error in both error criteria. Fig. 6 shows the accuracy of the developed models using the distorted layup scaling technique for predicting the fundamental frequency of the prototype along with the response that is predicted by applying the response scaling law Eq. (4.a). The selected cases 4, 5, 7, 10 and 16 also show the best predictions among all possible permutation cases. Although

the prototype layup includes ± 45 plies, none of the selected models has ± 45 plies in the layup, but each one still shows a very good accuracy in the prediction of the response of the prototype.

Table 1 lists the selected layups for the models with a total of 12 layers sorted by their corresponding error percentage in predicting the fundamental frequency of the prototype. The amount of error in the scaling law as shown in Fig. 5 for all 34 layups is related to the accuracy in predicting the fundamental frequency by each layup shown in Fig. 6. The layups that have less total error in satisfying the design scaling laws exhibit less discrepancy in the prediction of the fundamental frequency of the prototype, as is shown in Fig. 6.

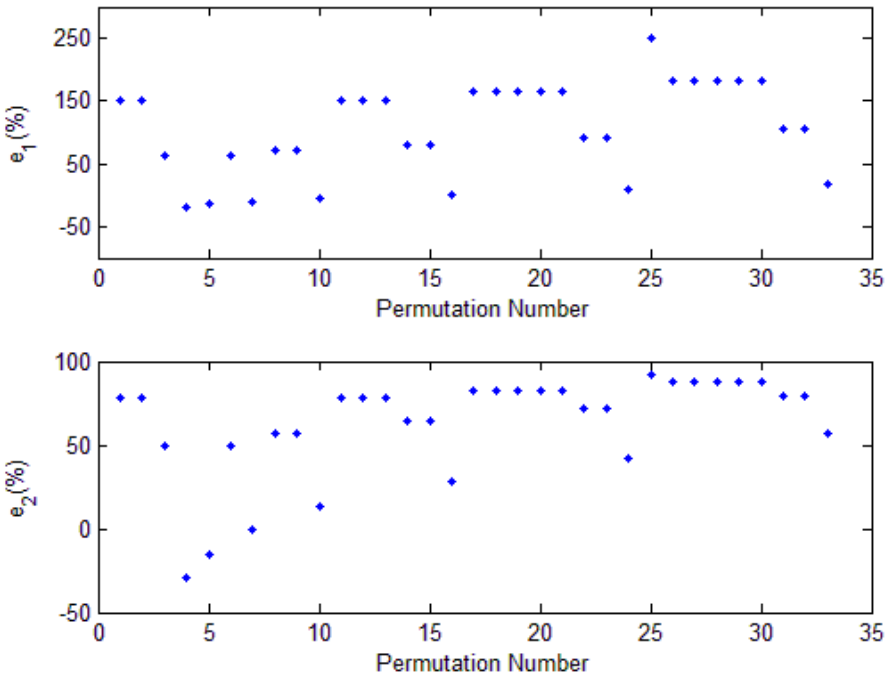

Fig. 5. The respective error percentages (defined by Eqs. 11a-b) for all possible ply schemes for the symmetric and balanced models with a total of 12 layers that only include 0, 90 and ± 45 plies for the prototype layup $[\pm 45_{\,2}/0_{\,46}]_s$.

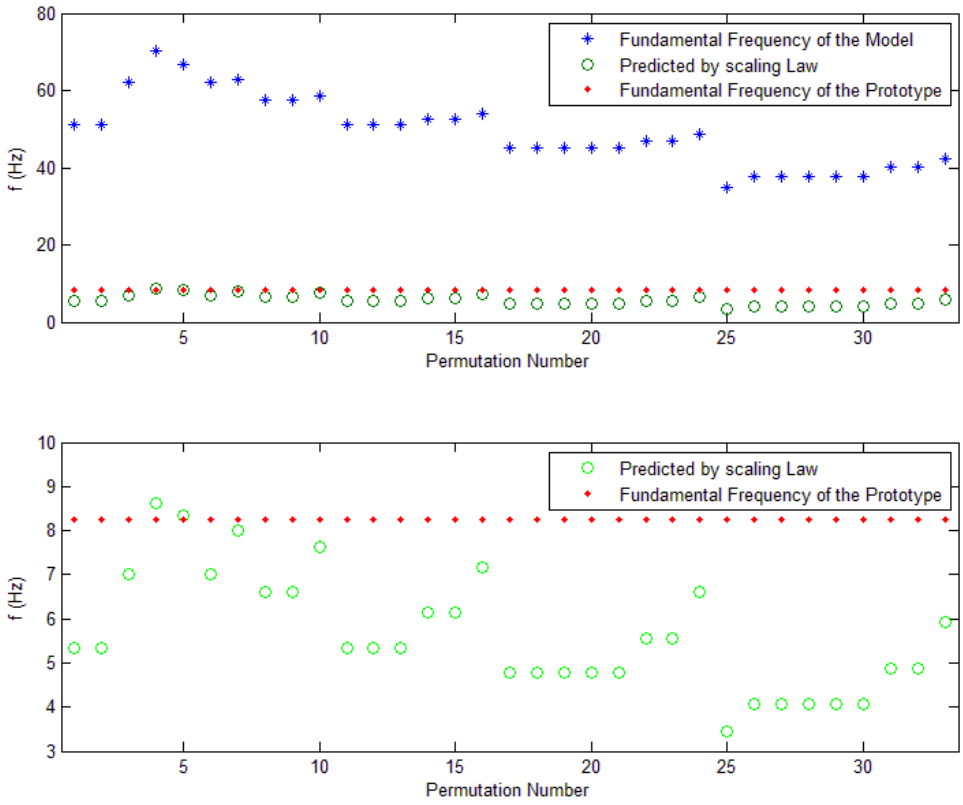

Fig. 6. Top: comparison of the predicted fundamental frequency of the prototype (green circles) to the actual frequency (red diamond) by using the fundamental frequency of the model (blue star) via the response scaling law for partial similarity (models with 12 layers) for the prototype layup $[\pm 45_{\ 2}/0_{\ 46}]_s$; Bottom: zoom in for the region that has predicted values.

Table 1. Selected ply schemes for the symmetric models with a total of 12 layers that only include 0, 90 and ± 45 plies for the prototype layup $[\pm 45_{\ 2}/0_{\ 46}]_s$.

Layup	Permutation Number	$e_1(\%)$	$e_2(\%)$	$e(\%)$	Error in predicting fundamental frequency (%)
$[0_{\ 5}/\ 90]_s$	5	-14.2	-15.0	2.9	1.2
$[0_{\ 4}/\ 90_{\ 2}]_s$	7	-9.4	-0.7	6.2	2.8
$[0_{\ 12}]$	4	-18.5	-29.4	11.4	4.5
$[0_{\ 3}/\ 90_{\ 3}]_s$	10	-4.0	13.6	16.0	8.0
$[0_{\ 2}/\ 90_{\ 4}]_s$	16	2.0	27.9	26.9	14.9

The approach was then applied to eight layers and $\lambda_l = 12.5$, i.e. 100 plies/8 = 12.5. The errors as defined by Eqs. (11a-b) for all of the possible symmetric and balanced 8-ply schemes for the models that only include 0, 90 and ± 45 plies is shown in Fig. 7. Among the 12 unique possibilities, the cases with permutation numbers 2, 3 and 5 were found to exhibit less than 30% error in both error criteria. Fig. 8 shows the accuracy of all the potential models using the distorted layup scaling technique in predicting the fundamental frequency of the prototype along with the response that is predicted by applying the scaling law Eq. (4.a). The selected cases with permutation numbers 2, 3 and 5 also show the best predictions among all other potential models.

Table 2 shows a list of the selected layups for the models with a total of eight layers. As shown in Table 2, layups with less amount of error in satisfying design scaling laws predict the fundamental frequency of the prototype more accurately. Also, the

total number of possible cases is less than the previous case study because the total number of layers considered for the models in this case is fewer (8 layers) which results in fewer permutations.

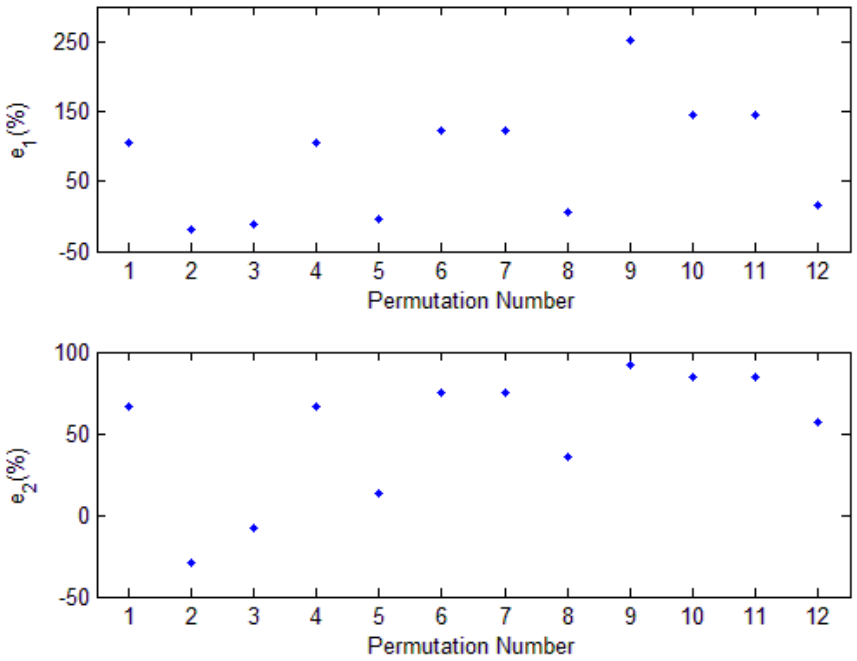

Fig. 7. Error percentage (defined by Eqs. 11a-b) for all possible ply schemes for the symmetric models with a total of 8 layers that only include 0, 90 and ± 45 plies for the prototype layup $[\pm 45_2/0_{46}]_s$.

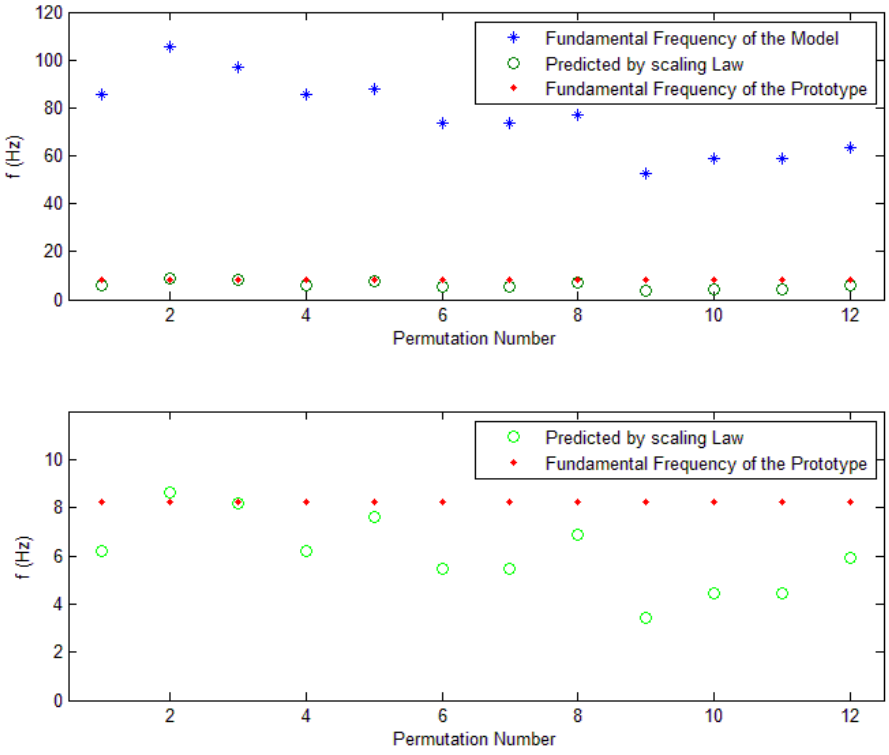

Fig. 8. Top: comparison of the predicted fundamental frequency of the prototype (green circles) to the actual frequency (red diamond) by using the fundamental frequency of the model (blue star) via the response scaling law for partial similarity (models with 8 layers) for the prototype layup $[\pm 45_{\,2}/0_{\,46}]_s$; Bottom: zoom in for the region that has predicted values.

Table 2. Selected ply schemes for the symmetric models with a total of 8 layers that only include 0, 90 and ± 45 plies for the prototype layup $[\pm 45_{\,2}/0_{\,46}]_s$.

Layup	Permutation Number	e_1(%)	e_2(%)	e (%)	Error in predicting fundamental frequency (%)
$[0_{\,3}/\,90]_s$	3	-11.8	-7.8	1.5	0.6
$[0_{\,8}]$	2	-18.5	-29.4	11.4	4.6
$[0_{\,2}/\,90_{\,2}]_s$	5	-4.0	13.6	16.0	8.0

Extending the analysis to an even smaller size having a total of six layers and $\lambda_l = 16.66$, i.e. 100 plies/6 = 16.33, were also investigated. Fig. 9 shows the value of the error criteria defined by Eq. (11a-b) for all possible symmetric and balanced layup for models with a total of six layers that only include 0, 90 and ± 45 plies. Among six possible cases, the cases with permutation numbers 2 and 1 were found with less than 30% error in both error criteria. Fig. 10 shows the accuracy of all the potential models using the distorted layup scaling technique in predicting the fundamental frequency of the prototype along with the response that is predicted by applying scaling law Eq. (4.a). The selected cases with permutation numbers 2 and 1 also show the best predictions among all other potential models. Table 3 shows a list of selected layups for the models with a total of six layers.

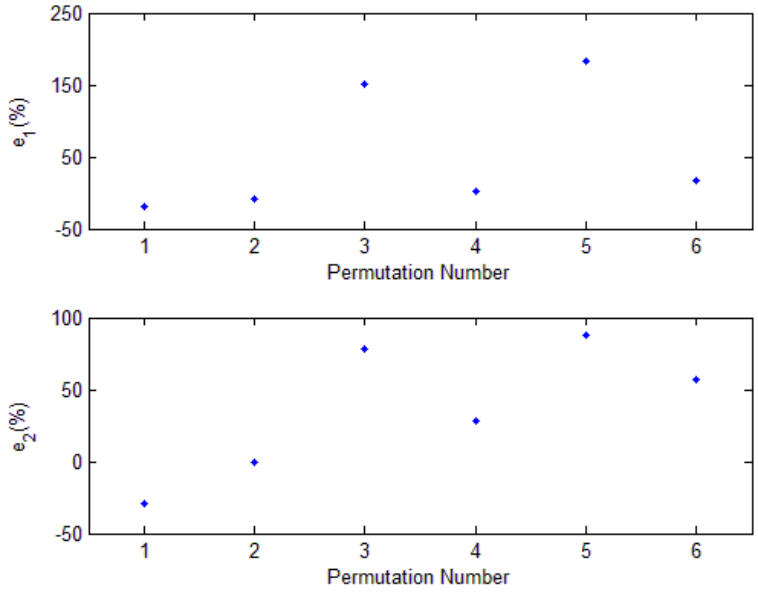

Fig. 9. Error percentage (defined by Eqs. 11a-b) for all possible ply schemes for the symmetric models with a total of 6 layers that only include 0, 90 and ± 45 plies for the prototype layup $[\pm 45_{\,2}/0_{\,46}]_s$.

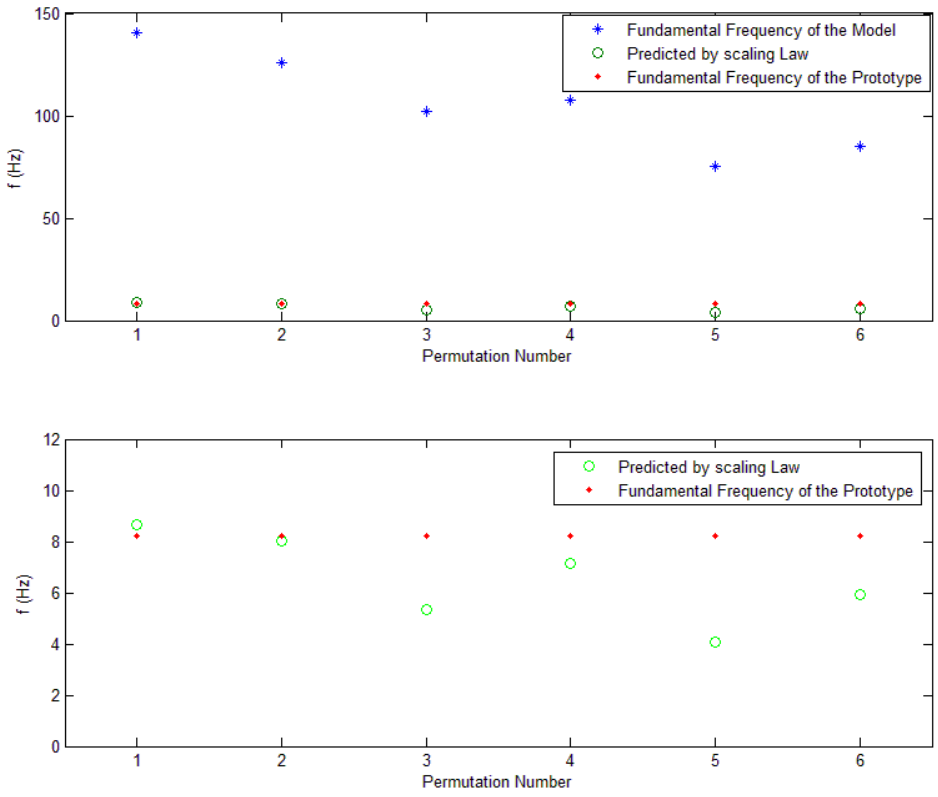

Fig. 10. Top: comparison of the predicted fundamental frequency of the prototype (green circles) to the actual frequency (red diamond) by using the fundamental frequency of the model (blue star) via the response scaling law for partial similarity (models with 6 layers) for the prototype layup $[\pm 45_{\,2}/0_{\,46}]_s$; Bottom: zoom in for the region that has predicted values.

Table 3. Selected ply schemes for the symmetric models with a total of six layers that only include 0, 90 and ± 45 plies for the prototype layup $[\pm 45_{\,2}/0_{\,46}]_s$.

Layup	Permutation Number	$e_1(\%)$	$e_2(\%)$	e (%)	Error in predicting fundamental frequency (%)
$[0_{\,2}/90]_s$	2	-9.4	-0.7	6.2	2.8
$[0_{\,6}]$	1	-18.5	-29.3	11.4	4.5

To further demonstrate the applicability of the proposed approach, a $[90_{\,2}/0_{\,46}]_s$ prototype layup was considered as an alternative and the same analysis was persued. Models in three different length scales with a total 12, 8 and 6 plies (e.g. $\lambda_l = 8.33$, $\lambda_l = 12.5$ and $\lambda_l = 16.66$, respectively) were developed. For each length scale, the models that were on the lower end of discrepancy in satisfying the design scaling laws were selected. Table 4 lists the selected layups for models with different length scales and their corresponding error values with respect to the design scaling laws. Fig. 11-13 show the accuracy of the predicted frequency with all of the possible layups for models with 12, 8 and 6 plies respectively. The selected layups listed in Table 4 demonstrated the least errors in satisfying the design scaling laws and also the least discrepancy in predicting the fundamental frequency of the prototype.

Table 4. Selected ply schemes for symmetric and balanced models with a total of 12, 8 and 6 layers that only include 0, 90 and ± 45 plies for the prototype layup $[90_{\,2}/0_{\,46}]_s$.

Layup		Permutation Number	$e_1(\%)$	$e_2(\%)$	e (%)	Error in predicting fundamental frequency (%)
$\lambda_l = 8.33$	$[0_{\,12}]$	4	-2.4	-5.6	3.7	1.5

	$[0_5/90]_s$	5	2.7	6.0	4.1	1.8
	$[0_4/90_2]_s$	7	8.5	17.7	12.6	6.0
	$[0_3/90_3]_s$	10	14.9	29.5	21.8	11.4
$\lambda_l = 12.5$	$[0_8]$	2	-2.4	-5.6	3.7	1.5
	$[0_3/90]_s$	3	5.5	11.9	8.3	3.8
	$[0_2/90_2]_s$	5	14.9	29.5	21.8	11.4
$\lambda_l = 16.66$	$[0_6]$	1	-2.4	-5.6	3.7	1.5
	$[0_2/90]_s$	2	8.5	17.7	12.6	6.0

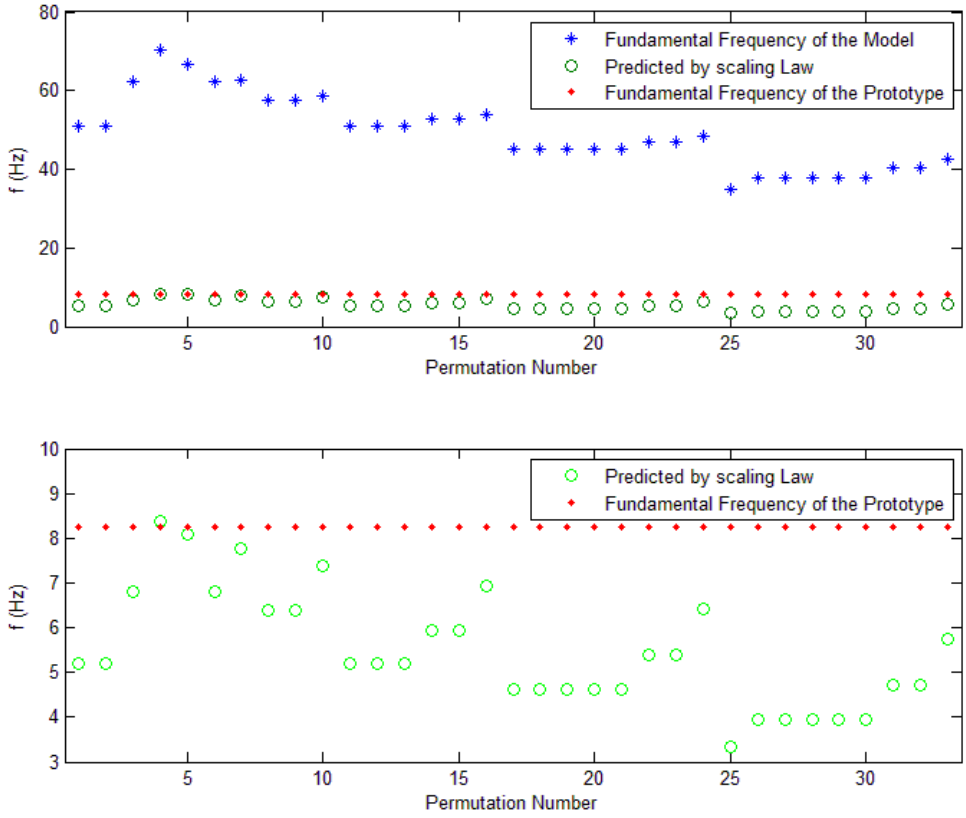

Fig. 11. Top: comparison of the predicted fundamental frequency of the prototype (green circles) to the actual frequency (red diamond) by using the fundamental frequency of the model (blue star) via the response scaling law for partial similarity (models with 12 layers) for the prototype layup $[90_2/0_{46}]_s$; Bottom: zoom in for the region that has predicted values.

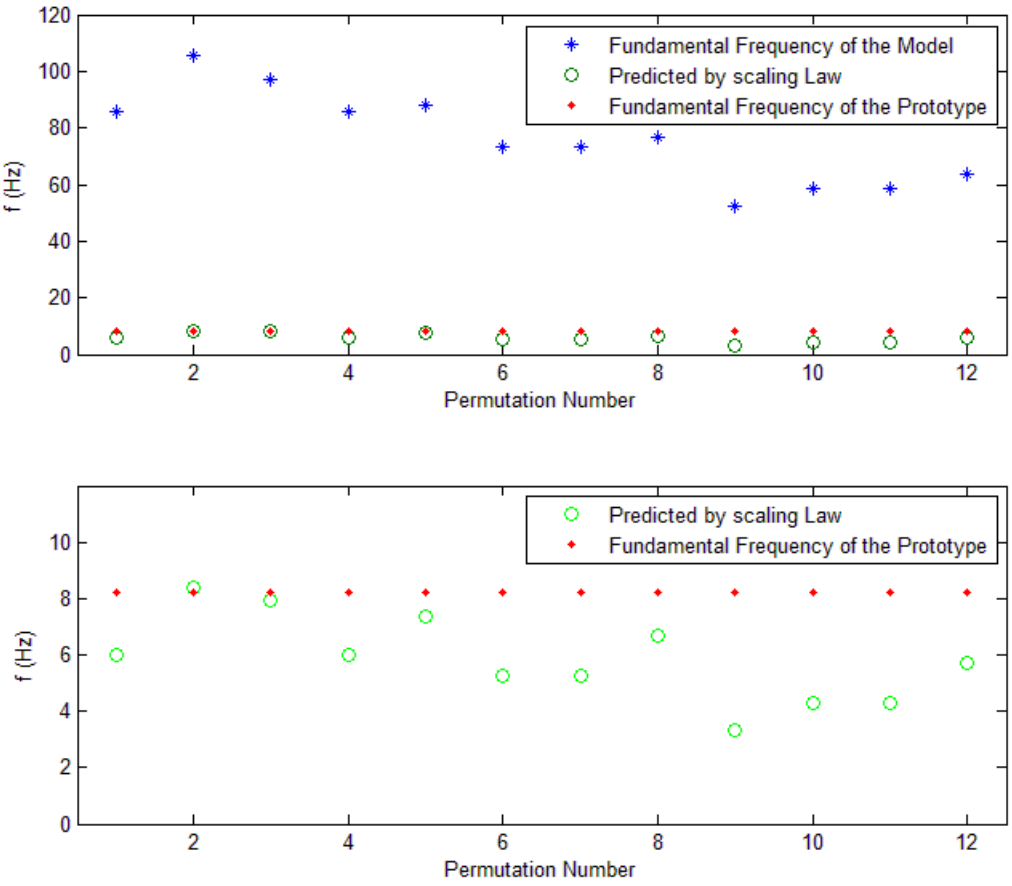

Fig. 12. Top: comparison of the predicted fundamental frequency of the prototype (green circles) to the actual frequency (red diamond) by using the fundamental frequency of the model (blue star) via the response scaling law for partial similarity (models with 8 layers) for the prototype layup $[90_2/0_{46}]_s$; Bottom: zoom in for the region that has predicted values.

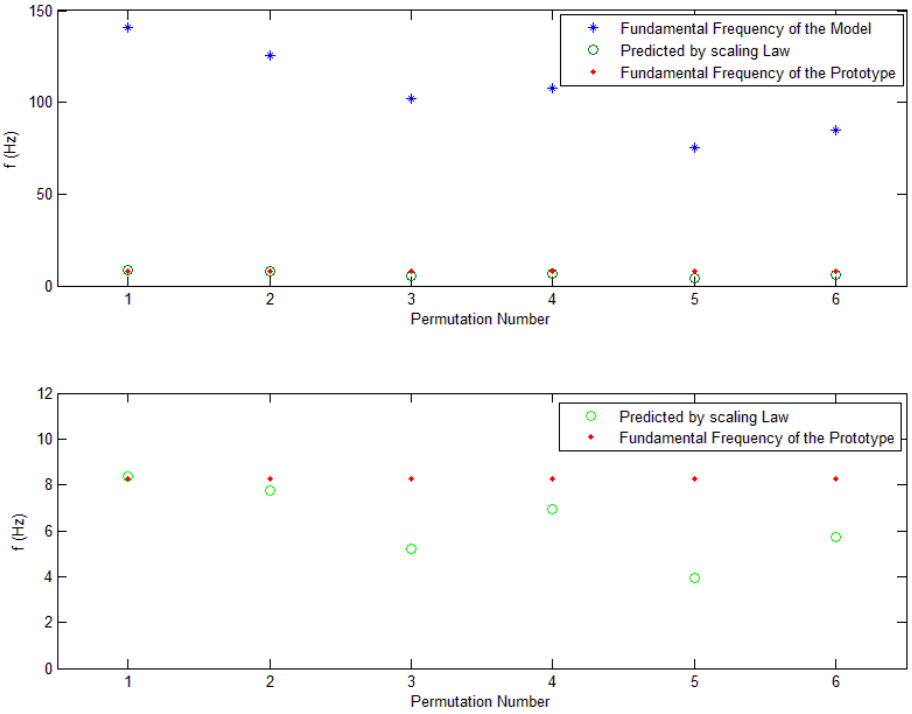

Fig. 13. Top: comparison of the predicted fundamental frequency of the prototype (green circles) to the actual frequency (red diamond) by using the fundamental frequency of the model (blue star) via the response scaling law for partial similarity (models with 6 layers) for the prototype layup $[90_2/0_{46}]_s$; Bottom: zoom in for the region that has predicted values.

6. Discussion

Eqs. (9) and (10) are the design scaling laws that need to be satisfied for complete similarity between the porotype and the scaled model. Eq. (9) can be easily satisfied by designing scaled models that have the same geometrical aspect ratios as the prototype. Eq. (10) depends on the proportionality of the extensional stiffness elements between the prototype and the model. Because the extensional stiffness of a laminate is not dependent on the position of its plies, changing the position of the plies in a developed model does not result in a different model. This fact limits the total number of the possible permutations because shuffling the plies in the flanges does not generate a new model in this study. Based on this observation, the number of the 0, 90 and ± 45 plies in each flange of the I-beam was varied to develop different models instead of changing the position of the plies in flanges.

Layup of the prototype has a critical role in design of its scaled models. The ply layup scheme of the prototype dictates whether the scaled models will exhibit complete or partial similarity. Assuming a unidirectional layup for the prototype, the ply-level scaling technique resulted in models with also a unidirectional layup that were completely similar to the prototype and showed an excellent ability to predict the frequency using the derived scaling laws. For the prototypes with a non-unidirectional layup, e.g. the $[\pm 45_2/0_{46}]_s$ and $[90_2/0_{46}]_s$ layups considered in this paper, the Distorted Layup Scaling technique resulted in partially similar models in different size scales with very good predictions of the fundamental frequencies of their respective prototypes. Based on the results presented in Tables 1 through 4, the models with less error in satisfying the design scaling laws show more accurate prediction of the prototype frequency. Selected models with less than 30% error in both e_1 and e_2 criteria show less than 15% discrepancy in prediction of the fundamental frequency of the prototype. Although the two considered layups for the prototype are different in non-unidirectional stack of plies, the majority of their layups consist of the unidirectional plies which results in a very close flexural and shear stiffness values for both prototypes. The proposed method searches for models with equivalent extensional stiffness values compared to the prototype defined by Eq. (10). This explains the similarity of selected models for both prototypes shown in Tables 1-4. However the orders of the accuracy of the models in predicting the frequency of each prototype are slightly different.

The implementation of the permutation is critical for the partial similarity as it gives all the possible layups for the model. The error criteria are defined to find the layup that works best with the derived scaling laws and gives the least error in predicting the frequency of the prototype. Although the best layup for the partially similar models in this study shows 1.5% error in predicting the fundamental frequency of its prototype, the implementation of the permutation is still necessary to avoid the cases that yield significant error in prediction of the frequencies of the prototype using the derived scaling laws.

A summary of the results is shown in Table 5 that includes the layups and overall dimensions for the most accurate developed models and their corresponding prototypes. As the total number of the layers for a model decreases, the probability to find a model which works well with the response scaling laws Eq. (4a-b) to predict the frequency of the prototype decreases. This decrease implies that there is a practical limit to the level of scaling that can be achieved when using the proposed Distorted Layup Scaling technique for laminated structures. Although the proposed approach was investigated for specific laminated I-beams as the prototype, it can be applied to prototypes with other geometries and layups. If accurate governing equations can be found for the laminated prototype, then the Distorted Layup Scaling technique can be applied to develop partially similar models that predict the natural frequencies of the prototype.

Table 5. Different case studies were conducted using complete and partial similarity for the I-beam.

Category	Type	Layup	Total number of the plies	$b_1 = b_2 = b_3$ (m)	Length (m)
Complete Similarity	Prototype	$[0\,]_{100}$	100	2.446	29.3
	Models	$[0\,]_n$; n=1-100	1-100	0.02446-2.446	0.293-29.3
Partial Similarity (Case 1)	Prototype	$[\pm 45_{\,2}/0_{\,46}]_s$	100	2.446	29.3
	Models	$[0_{\,5}/\,90]_s, [0_{\,4}/\,90_{\,2}]_s$	12	0.29352	3.516
	Models	$[0_{\,3}/\,90]_s, [0_{\,8}]$	8	0.19568	2.344
	Models	$[0_{\,2}/\,90]_s, [0_{\,6}]$	6	0.14676	1.758
Partial Similarity (Case 2)	Prototype	$[90_{\,2}/0_{\,46}]_s$	100	2.446	29.3
	Models	$[0_{\,12}], [0_{\,5}/\,90]_s$	12	0.29352	3.516
	Models	$[0_{\,8}], [0_{\,3}/\,90]_s$	8	0.19568	2.344
	Models	$[0_{\,6}], [0_{\,2}/\,90]_s$	6	0.14676	1.758

7. Conclusion

Scaled-down models have the potential to facilitate and to expedite the certification of the new materials and alternative designs for wind turbine blades. To demonstrate this potential, theoretical study was pursued to design a scaled-down model replicating the dynamic characteristics of a representative I-beam structure inside a utility-scale wind turbine blade. Structural similitude theory was applied to the governing equations for vibration of a simply-supported shear deformable thin-walled composite I-beam to derive the scaling laws. Effects of the geometry and layup on accuracy of the designed models in predicting the fundamental frequency of the prototype were investigated for both complete- and partial-similarity cases. The ply-level scaling technique was used to develop scaled models that are completely similar to a unidirectional-only ply-stackup prototype. The Distorted Layup Scaling approach was proposed to design partially-similar scaled-down models with layups different from the layup of their corresponding prototype. Then, the accuracy of the designed models was investigated by predicting the fundamental frequency of prototype using the response scaling laws. According to the results, scaled-down I-beams with different size scales were designed which could predict the fundamental frequency of their corresponding prototype with a very good accuracy.

Acknowledgments

This material is based upon work supported by the National Science Foundation under Grant Number 1230884 (Achieving a Sustainable Energy Pathway for Wind Turbine Blade Manufacturing). Any opinions, findings, and conclusions or recommendations expressed in this material are those of the author(s) and do not necessarily reflect the views of the National Science Foundation.

References

[1] Mandell JF, Combs DE, Samborsky DD. Fatigue of fiberglass beam substructures. Wind Energy. 1995;16:99.

[2] Cairns DS, Skramstad JD, Mandell JF. Evaluation of hand lay-up and resin transfer molding in composite wind turbine blade structures. International SAMPE Symposium and Exhibition: SAMPE; 1999. p. 967-80.

[3] Mandell JF, Creed Jr RJ, Pan Q, Combs DW, Shrinivas M. Fatigue of fiberglass generic materials and substructures. Wind Energy. 1994:207.

[4] Sayer F, Post N, Van Wingerde A, Busmann HG, Kleiner F, Fleischmann W, et al. Testing of adhesive joints in the wind industry. European Wind Energy Conference and Exhibition 2009, EWEC 2009. p. 288-315.

[5] Sayer F, Antoniou A, Van Wingerde A. Investigation of structural bond lines in wind turbine blades by sub-component tests. International Journal of Adhesion and Adhesives. 2012;37:129-35.

[6] Zarouchas DS, Makris AA, Sayer F, Van Hemelrijck D, Van Wingerde AM. Investigations on the mechanical behavior of a wind rotor blade subcomponent. Composites Part B: Engineering. 2012;43:647-54.

[7] Jensen FM, Falzon BG, Ankersen J, Stang H. Structural testing and numerical simulation of a 34 m composite wind turbine blade. Composite Structures. 2006;76:52-61.

[8] White D, Musial WD, Engberg S, Embry-Riddle Aeronautical U, National Renewable Energy L. - Evaluation of the New B-REX Fatigue Testing System for Multi-megawatt Wind Turbine Blades: Preprint. - National Renewable Energy Laboratory; 2005.

[9] Simitses GJ, Rezaeepazhand J. Structural similitude for laminated structures. Composites Engineering. 1993;3:751-65.

[10] Rezaeepazhand J, Simitses GJ. Use of scaled-down models for predicting vibration response of laminated plates. Composite Structures. 1995;30:419-26.

[11] Rezaeepazhand J, Simitses GJ, Starnes Jr JH. Design of scaled down models for stability of laminated plates. AIAA journal. 1995;33:515-9.

[12] Simitses GJ, Rezaeepazhand J. Structural similitude and scaling laws for buckling of cross-ply laminated plates. Journal of Thermoplastic Composite Materials. 1995;8:240-51.

[13] Rezaeepazhand J, Simitses GJ, Starnes Jr JH. Design of scaled down models for predicting shell vibration response. Journal of Sound and Vibration. 1996;195:301-11.

[14] Rezaeepazhand J, Simitses GJ. Structural similitude for vibration response of laminated cylindrical shells with double curvature. Composites Part B: Engineering. 1997;28:195-200.

[15] Asl ME, Niezrecki C, Sherwood J, Avitabile P. Predicting the vibration response in subcomponent testing of wind turbine blades. Special Topics in Structural Dynamics, Volume 6: Springer; 2015. p. 115-23.

[16] Asl ME, Niezrecki C, Sherwood J, Avitabile P. Application of structural similitude theory in subcomponent testing of wind turbine blades. Proceedings of the American Society for Composites. 2014:8-10.

[17] Asl ME, Niezrecki C, Sherwood J, Avitabile P. Similitude Analysis of Composite I-Beams with Application to Subcomponent Testing of Wind Turbine Blades. Experimental and Applied Mechanics, Volume 4: Springer; 2016. p. 115-26.

[18] Vo TP, Lee J. Flexural–torsional coupled vibration and buckling of thin-walled open section composite beams using shear-deformable beam theory. International Journal of Mechanical Sciences. 2009;51:631-41.

[19] Griffith DT, Ashwill TD. The Sandia 100-meter all-glass baseline wind turbine blade: SNL100-00. Sandia National Laboratories, Albuquerque, Report NoSAND2011-3779. 2011.

[20] Cortínez V, Piovan M. Vibration and buckling of composite thin-walled beams with shear deformability. Journal of Sound and Vibration. 2002;258:701-23.

[21] Reddy JN. Mechanics of laminated composite plates and shells : theory and analysis. Boca Raton, Fla.; London: CRC, 2003.

[22] Piovan MT, Cortínez VH. Transverse shear deformability in the dynamics of thin-walled composite beams: consistency of different approaches. Journal of Sound and Vibration. 2005;285:721-33.